NUKLEONIKA 2006;51(Supplement 1):S11–S18

Design of high quality doped CeO_2 solid electrolytes with nanohetero structure

Toshiyuki Mori,
John Drennan,
Ding R. Ou,
Fei Ye

Abstract Doped ceria (CeO_2) compounds are fluorite related oxides which show oxide ionic conductivity higher than yttria-stabilized zirconia in oxidizing atmosphere. As a consequence of this, a considerable interest has been shown in application of these materials for low (400–650°C) temperature operation of solid oxide fuel cells (SOFCs). In this paper, our experimental data about the influence of microstructure at the atomic level on electrochemical properties were reviewed in order to develop high quality doped CeO_2 electrolytes in fuel cell applications. Using this data in the present paper, our original idea for a design of nanodomain structure in doped CeO_2 electrolytes was suggested. The nanosized powders and dense sintered bodies of M doped CeO_2 (M:Sm,Gd,La,Y,Yb, and Dy) compounds were fabricated. Also nanostructural features in these specimens were introduced for conclusion of relationship between electrolytic properties and domain structure in doped CeO_2. It is essential that the electrolytic properties in doped CeO_2 solid electrolytes reflect in changes of microstructure even down to the atomic scale. Accordingly, a combined approach of nanostructure fabrication, electrical measurement and structure characterization was required to develop superior quality doped CeO_2 electrolytes in the fuel cells.

Key words doped CeO_2 • oxide ionic conductivity • microdomain • low temperature operation of fuel cells application • nanohetero structure • domain structure

T. Mori✉, D. R. Ou, F. Ye
Ecoenergy Materials Group,
Ecomaterials Center,
National Institute for Materials Science,
1-1 Namiki, Tsukuba, Ibaraki 305-0044, Japan,
Tel.: +81 29 860 4395, Fax: +81 29 852 7449,
E-mail: MORI.Toshiyuki@nims.go.jp

J. Drennan
Center for Microscopy and Microanalysis,
The University of Queensland,
St. Lucia, Brisbane, Qld 4072, Australia

Received: 20 October 2005
Accepted: 6 December 2005

Introduction

Over the past 40 years, the potential of materials with fast oxide ionic conduction has been realized in many applications. Oxide ion conductors are used in a variety of gas sensors, [29] solid oxide electrochemical cells (SOECs), [6] and solid oxide fuel cells (SOFCs) [10, 21]. In these applications, SOFCs are being especially developed as a clean and efficient power source for generating electricity from a variety of fuels. For long lifetimes with low temperature (400–650°C) and efficient operation below 500°C, high oxide ionic conductivity is required for the electrolytes. The low temperature operation of SOFCs means that less expensive materials can be used as interconnects, manifolds and gas transport systems. Yttria stabilized zirconia (YSZ) and scandia stabilized zirconia (SSZ) are common electrolytes used in SOFCs [10, 28]. However, its ionic conductivity is still unsatisfactory for low temperature operation of SOFCs. Accordingly, it is important that a high-quality electrolyte with higher oxide ionic conductivity than that of YSZ and SSZ be identified.

CeO_2 doped with the oxides of di- or trivalent metal oxides such as calcia (CaO) or rare earth oxide doped CeO_2 possess higher oxide ionic conductivity than any reported stabilized zirconia [3, 20, 27]. At high oxygen partial pressures, these doped CeO_2 electrolytes show high oxide ionic conductivity. At low oxygen partial

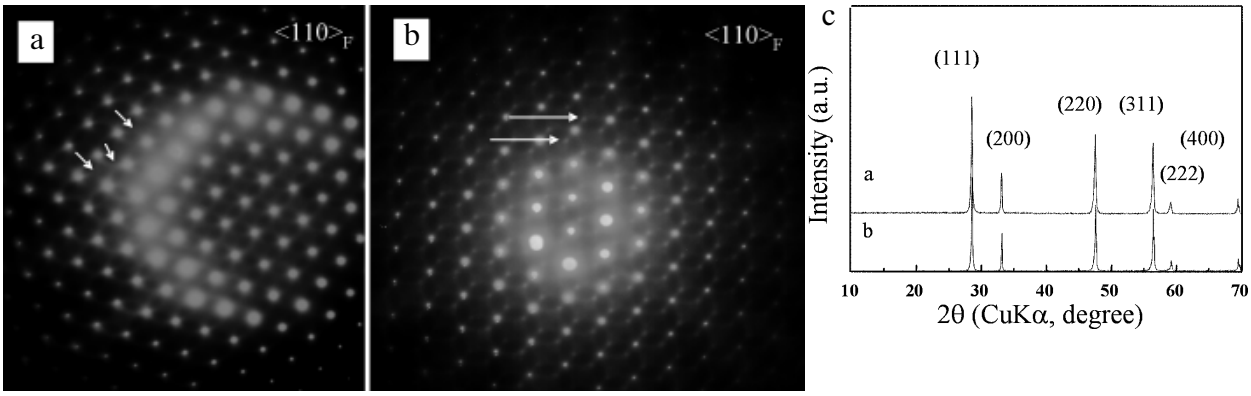

Fig. 1. Selected area electron diffraction patterns and X-ray diffraction profiles recorded from (a) $Y_{0.15}Ce_{0.85}O_{1.925}$ and (b) $Y_{0.25}Ce_{0.75}O_{1.875}$. Arrow symbols indicate the extra reflections. (c) X-ray diffraction patterns recorded from specimens (a) and (b). Ref. [13].

pressures associated with anodic conditions, however, the Ce^{4+} ion can be partially reduced to Ce^{3+} ion in doped CeO_2. Quasi-free electrons are introduced into a fluorite lattice in such reducing atmospheres. Doped CeO_2 compounds are partially reduced and develop electronic conductivity under anodic conditions in the fuel cell. The stability in both oxidizing and reducing atmosphere is an essential requirement for candidate electrolytes rare earth doped CeO_2 systems. To overcome this problem and improve the conductivity for low temperature operation of SOFCs, a design of nanostructure in doped CeO_2 solid electrolytes is required. In this paper, the authors introduce our recent data for a microanalysis in the doped CeO_2 electrolytes and suggest a strategy to improve the conductivity of doped CeO_2 electrolytes for application in solid oxide fuel cell systems. We expect that both the control of processing route of doped CeO_2 ceramics and the atom-level observation of the microstructure in the doped CeO_2 solid electrolytes will clarify the best pathway for development of high quality doped CeO_2 solid electrolytes.

Microstructure and microanalysis of doped CeO_2 electrolytes

Influence of dopant content on electrolytic properties of CeO_2 electrolytes doped with rare earth oxide or alkaline earth oxide has been widely investigated. The additives produce materials with extensive solid solubility in the fluorite CeO_2 lattice. The relationship among electrochemical properties, dopant size, and dopant concentration in CeO_2 electrolytes was widely investigated before [2, 8]. It has been considered that the aforementioned doped CeO_2 electrolytes exhibited high oxide ionic conductivity due to the small association enthalpy between dopant cation and oxygen vacancy in the fluorite lattice. However, these arguments lacked microanalysis in doped CeO_2 electrolytes. The prospective improvements in the conductivity of doped CeO_2 would be limited. In light of this limitation, a careful atom level observation is required for development of doped CeO_2.

The author examined the relationship among oxide ionic conductivity, dopant content and microstructural features of Y doped CeO_2 electrolyte [13, 18]. The conductivity show the maximum at the composition around $x = 0.15$ in $Y_xCe_{1-x}O_{2-x/2}$ ($x = 0.15$, 0.2 and 0.25) system. Also, the activation energy of Y doped CeO_2 electrolytes was minimized at the same composition. This indicates that the mobility of oxide ion maximized at the aforementioned composition in the $Y_xCe_{1-x}O_{2-x/2}$ system. To conclude why the conductivity and activation energy have optimum value in Y doped CeO_2, the crystal phase and nanostructural feature in the sintered bodies were examined.

The selected area electron diffraction patterns (SAEDPs) recorded from $Y_xCe_{1-x}O_{2-x/2}$ ($x = 0.15$, and 0.25) sintered bodies have extra reflections (Fig. 1), although the X-ray diffraction profiles recorded from these sintered bodies consist of simple fluorite phase (Fig. 1). Also the diffuse scattering appears around the extra reflection in the SAEDPs. The intensity of extra reflection and diffuse scattering in SAEDP of $Y_{0.25}Ce_{0.75}O_{1.875}$ is much stronger than that of $Y_{0.15}Ce_{0.85}O_{1.925}$. This indicates that both specimens have the microdomain with ordered structure of oxygen vacancy. The microdomain size in $Y_{0.25}Ce_{0.75}O_{1.875}$ is bigger than that in $Y_{0.15}Ce_{0.85}O_{1.925}$. To conclude the domain structure, the observed SAEDP was compared with the calculated one. Since the observed pattern almost agreed with calculated one, it is concluded that microdomain consists of distorted c-type rare earth structure. The position of calculated pattern was not exactly equal to that of observed pattern; however, it indicates that the domains did not consist of the simple solid solution of Y_2O_3. The domains would consist of a transitional phase with microstructure between fluorite CeO_2 and c-type rare earth Y_2O_3.

Figure 2 shows the high resolution TEM (HRTEM) images recorded from the typical grains in Y doped CeO_2 electrolytes. In $Y_{0.15}Ce_{0.85}O_{1.925}$ sample (Fig. 2a), dislocations (i.e. partial dislocation) and lattice distortions covered several atoms (as pointed by the arrows) were observed inside the matrix with fluorite structure. And this distortion formed a different structure as compared with the matrix in the grain (as enclosed by the dashed line). The distortion area in this specimen was enlarged to approximately 5 nm in dimension. Also the distortion would introduce the aforementioned dislocation around the domain. The domain size and

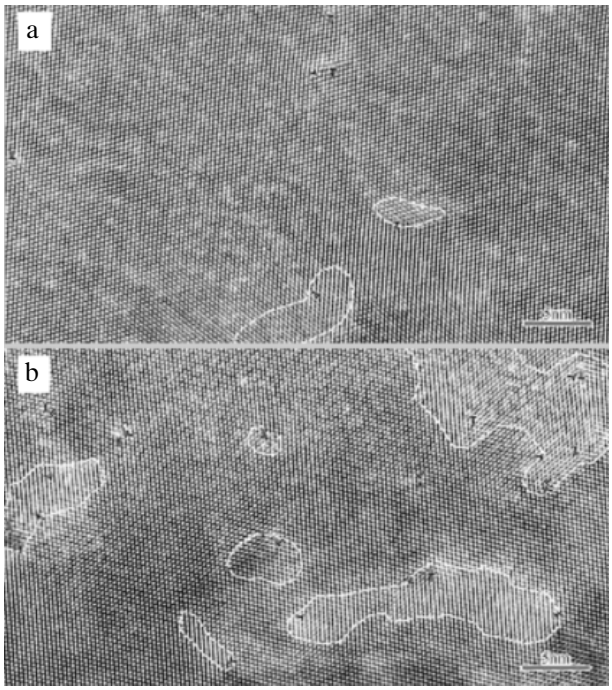

Fig. 2. High resolution image recorded from sintered bodies with the composition of (a) $x = 0.15$ and (b) $x = 0.25$ in $Y_xCe_{1-x}O_{2-x/2}$ system. Dashed line area means microdomain. Ref. [18].

domain content increased with increasing dopant concentration. The observed domain sizes were over 10 nm when the dopant concentration was 25 atom% (Fig. 2b). The high resolution images of the aforementioned specimens agree with the conclusion as shown in Fig. 1. And the dopant cations would aggregate together and precipitate from the matrix. The oxygen vacancies would be deeply trapped by these precipitates (i.e. microdomains) and be arranged with short-ranged orders in the matrix of CeO_2. Therefore, the authors concluded that the microdomain size and microdomain content influence the conducting properties of doped CeO_2. The big microdomain would lower the conducting properties in Y doped CeO_2 solid electrolytes.

Figure 3 presents the STEM analysis data and image analysis data of $Yb_{0.25}Ce_{0.75}O_{1.875}$ electrolytes [31]. Some darker areas in the bright field image (Fig. 3a) were brighter in the dark field image (Fig. 3b). Since the dark field image includes the information of both structure and composition, it is concluded that the chemical composition and crystal structure in the aforementioned areas are different from the matrix. The authors believed that these areas were microdomains observed by HRTEM. It is concluded that the microdomains contained higher concentration of dopant cation (i.e. Yb element) than that of the matrix. The composition difference between the microdomains and matrix in $Yb_{0.25}Ce_{0.75}O_{1.875}$ sintered specimen was further analyzed by energy filter TEM (EFTEM). This analysis indicates that Yb concentration in the microdomains was about 30–40 atm%, while that in the matrix was about 25 atm%. This suggests that the small amount of dopant cation is aggregated in the microdomain area. The authors concluded that the microdomain consisted of the distorted c-type structure. In the unit cell of c-type rare earth structure, there are four layers of oxygen atoms when the unit cell is viewed from <0,0,1> direction. The HRTEM images of 25 atm% Yb doped

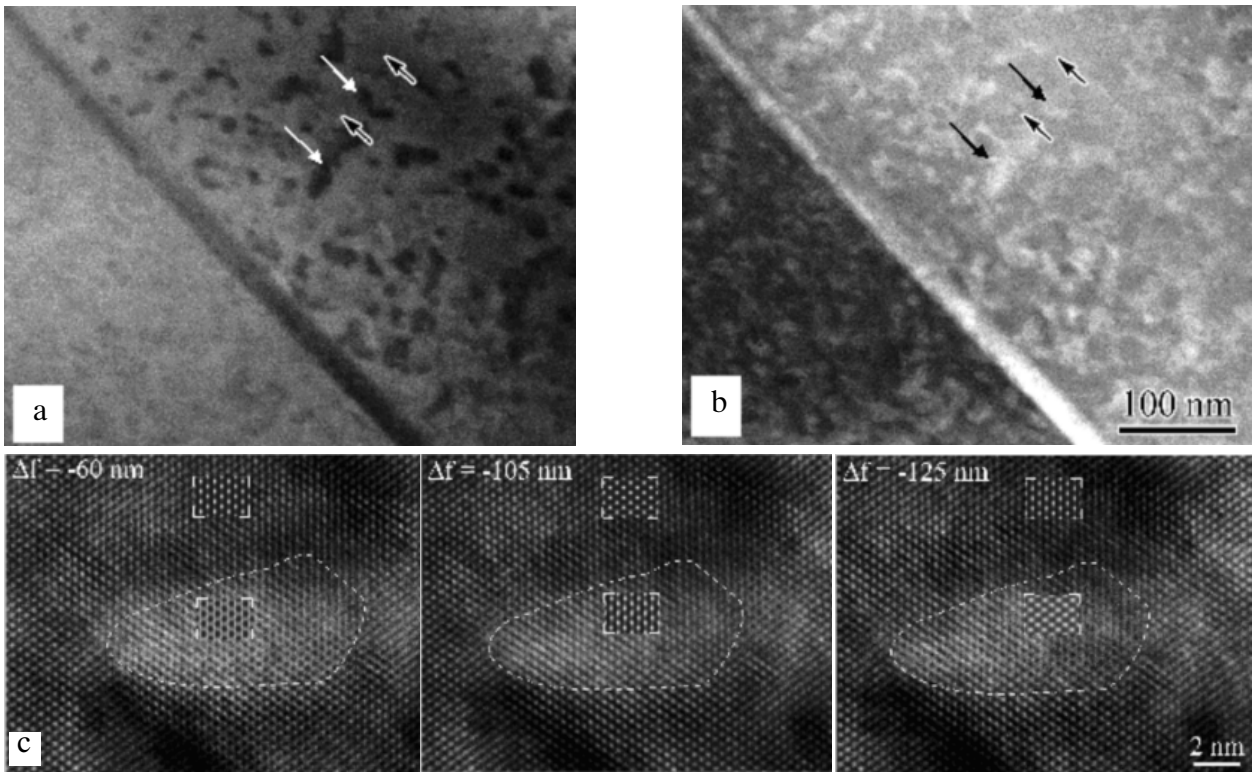

Fig. 3. STEM images and image analysis of $Yb_{0.25}Ce_{0.75}O_{1.875}$. a – Bright field image; b – dark field image; c – image analysis of HRTEM. Arrow symbols indicate the microdomains. Dashed line area is microdomain. Simulated image was inserted in the images. Ref. [30].

CeO_2 were simulated using the software Electron Microscopy Software Java Version (JEMS) as shown in Fig. 3c [30]. Since both microdomain and matrix consist of cubic structure, the orientation of the microdomains is the same as that of the matrix. Therefore, the matrix and microdomain are both viewed from <1,1,0> direction in Fig. 3c. Both images of matrix and microdomain in this figure are simulated and the simulated images are inserted. The lattice points of the microdomain appear as black spots when $\Delta f = -60$ nm. When $\Delta f = -105$ nm and -125 nm, the lattice points of microdomain appear as white spots. This indicates that microdomain area consists of layer structure of oxygen vacancy as well as c-type rare earth structure. The simulated images are consistent with the observations. On the other hand, the images of the matrix with different defocus are almost the same. This means that the matrix consists of fluorite structure without layer structure of oxygen vacancy. Therefore, our conclusion in Fig. 2 was re-confirmed by the image simulation of HRTEM.

The authors have been extensively investigated the influence of nanostructural features on conducting properties in Gd- [12], Sm- [11, 15, 17], or La doped CeO_2 electrolytes [11, 14, 15, 17]. In the case of $Sm_xCe_{1-x}O_{2-x/2}$ (x = 0.1, 0.15, 0.2, and 0.25) sintered bodies, the activation energy of Sm doped CeO_2 electrolytes was minimized at the composition around $x = 0.15$ in $Sm_xCe_{1-x}O_{2-x/2}$ system as well as Y- or Yb doped CeO_2 system. Also, the conductivity shows the maximum at the same composition. This indicates that the mobility of oxide ion maximized at the aforementioned composition in $Sm_xCe_{1-x}O_{2-x/2}$ system. To conclude why the conductivity and activation energy have optimum value in Sm doped CeO_2, the crystal phase and nanostructural feature in the sintered bodies were examined. The SAEDPs recorded from $Sm_{0.1}Ce_{0.9}O_{1.95}$ and $Sm_{0.25}Ce_{0.75}O_{1.875}$ sintered bodies have the extra reflections. The position of extra reflection was different from that in SAEDPs recorded from Y- or Yb doped CeO_2 (Fig. 4). Also the diffuse scattering appeared around the extra reflection in both specimens. This indicates that the microdomain structure in Sm doped CeO_2 is different from that in Y- or Yb doped CeO_2. It is found that the microdomain in Sm doped CeO_2 consists of distorted pylochlore structure by comparing observed SAEDPs with calculated one. And the intensity of extra reflection and diffuse scattering in SAEDP of $Sm_{0.25}Ce_{0.75}O_{1.875}$ with low conductivity were much stronger than that of $Sm_{0.15}Ce_{0.9}O_{1.95}$ with high conductivity. This indicates that both specimens include the microdomain with ordered structure of oxygen vacancy. The microdomain size in $Sm_{0.25}Ce_{0.75}O_{1.875}$ is bigger than that in $Sm_{0.15}Ce_{0.9}O_{1.95}$. The high resolution images of the aforementioned both specimens agreed with this conclusion. Therefore, we re-confirmed that the big microdomain lowers the conducting properties in the doped CeO_2 solid electrolytes. The relationship between conducting properties and nanostructural features in Gd doped CeO_2 is the same as that in Sm doped CeO_2. The microdomain in Gd doped CeO_2 consists of distorted pylochlore structure as well as that

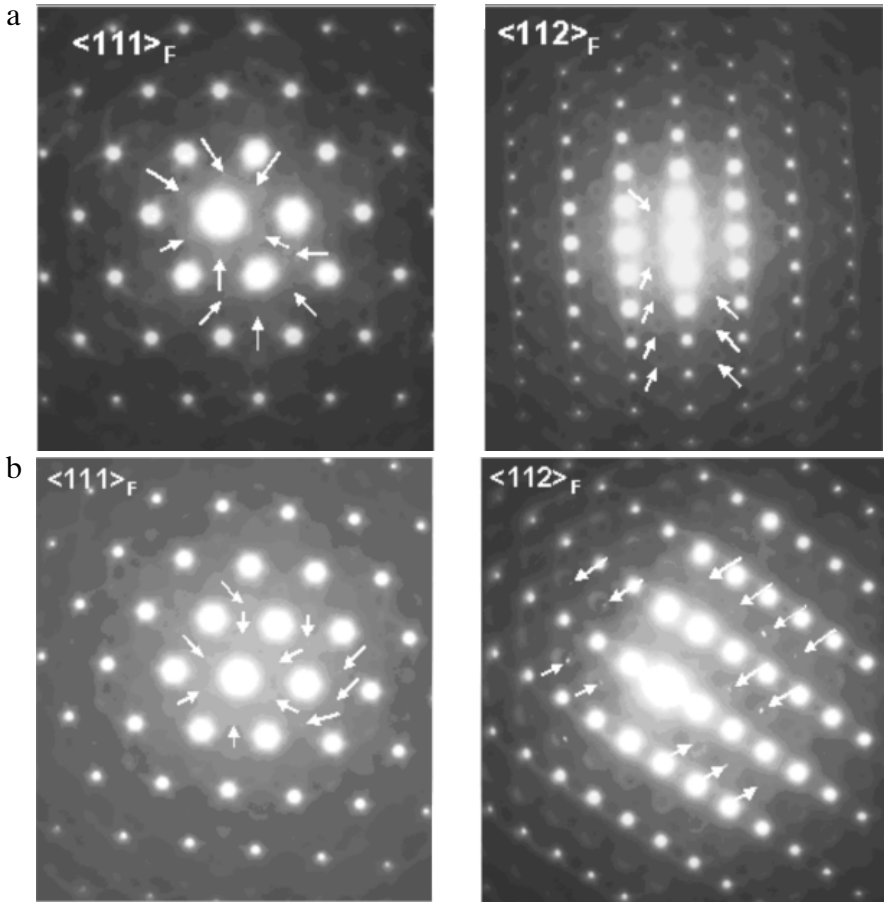

Fig. 4. Selected area electron diffraction patterns recorded from (a) $Sm_{0.15}Ce_{0.85}O_{1.925}$, and (b) $Sm_{0.25}Ce_{0.75}O_{1.875}$ sintered bodies. Arrow symbols indicate extra reflections.

of Sm doped CeO_2. The domain size (approx. 2 nm) in $Gd_{0.15}Ce_{0.85}O_{1.925}$ with high conductivity was much smaller than that (10 nm or more) in $Gd_{0.25}Ce_{0.75}O_{1.875}$. This concluded that the result in Gd doped CeO_2 system supports our conclusion again. It is obviously indicates that microdomain size should be minimized for development of high quality doped CeO_2 solid electrolytes.

The relationship between grain size and electrical conductivity for doped CeO_2 electrolytes has been investigated before [4, 5, 7, 20]. However, there are few papers that examine the microstructure of doped CeO_2 electrolytes in detail. One exception is the work of Gerhardt *et al*. [5] who investigated the grain boundary of Gd doped CeO_2 electrolyte using STEM technique. They observed the presence of thick grain boundaries and identified regions of amorphous SiO_2 rich phases. They suggested that the relatively large grain boundary resistivity of doped CeO_2 electrolytes was attributable to such siliceous thick film around grains of doped CeO_2. They concluded that the influence of grain size on grain boundary resistivity might be related to the siliceous thick film.

The authors have been examined the relationship among grain size, conducting properties and microstructure of Y- [18], Yb- [30], Gd- [1], Dy doped [24] CeO_2 electrolytes. Figure 5 shows the average grain size dependence of conductivity and the HRTEM images of typical grains in $Y_{0.25}Ce_{0.75}O_{1.875}$ samples with average grain size about 0.92 μm and 90 nm. Since the authors can prepare nanosized easy sinterable powders, the average grain size in the dense specimens can be control from 90 nm to 0.92 μm by selection of optimum sintering temperature from 900°C to 1450°C. The aforementioned two samples were corresponding to the $Y_{0.25}Ce_{0.75}O_{1.875}$ electrolytes with the maximum average grain size and the minimum average grain size in Fig. 5. In the grain size dependence of conductivity, the conductivity decreased with decreasing grain size and reached the lowest value at an average grain size of 300 nm. Also the activation energy increased with decreasing grain size and reached a maximum at the aforementioned average grain size. This tendency would be attributable to the space charge layer around the grain boundary in the sintered body. On the other hand, the conductivity increased with a decrease of grain size under 300 nm. In this region, it is concluded that the space charge layer with high resistivity is minimized around the grain boundary. Since the change of conductivity is large when the grains are below 300 nm, then we suggest it is not all attributable to space charge changes. Other microstructural features within the grain are also beginning to have an influence. Both change of the space charge layer width around the grain boundary and the microstructural features within the grain would lead to improve the conductivity, that are observed under 300 nm of grain size in the sintered bodies. In the image of HRTEM recorded from specimens with small grains, the grain boundary in both specimens was very clean. The microdomain size in the specimen with big grain and low conductivity is much bigger than that in the specimen with small grains and high conductivity. The microdomains in the specimen with small grain size were rarely observed using TEM analysis. This suggests that the heterogeneity of microstructure in the grain was lowered by low temperature sintering. It is concluded that low temperature sintering minimizes the microdomain size in the grain and improves the conducting property in the specimen. While this microstructural change is subtle, the nanohetero structure with microdomain in the grain has a significant influence on the electrolytic properties. To conclude the grain size dependence of conducting property in detail, the

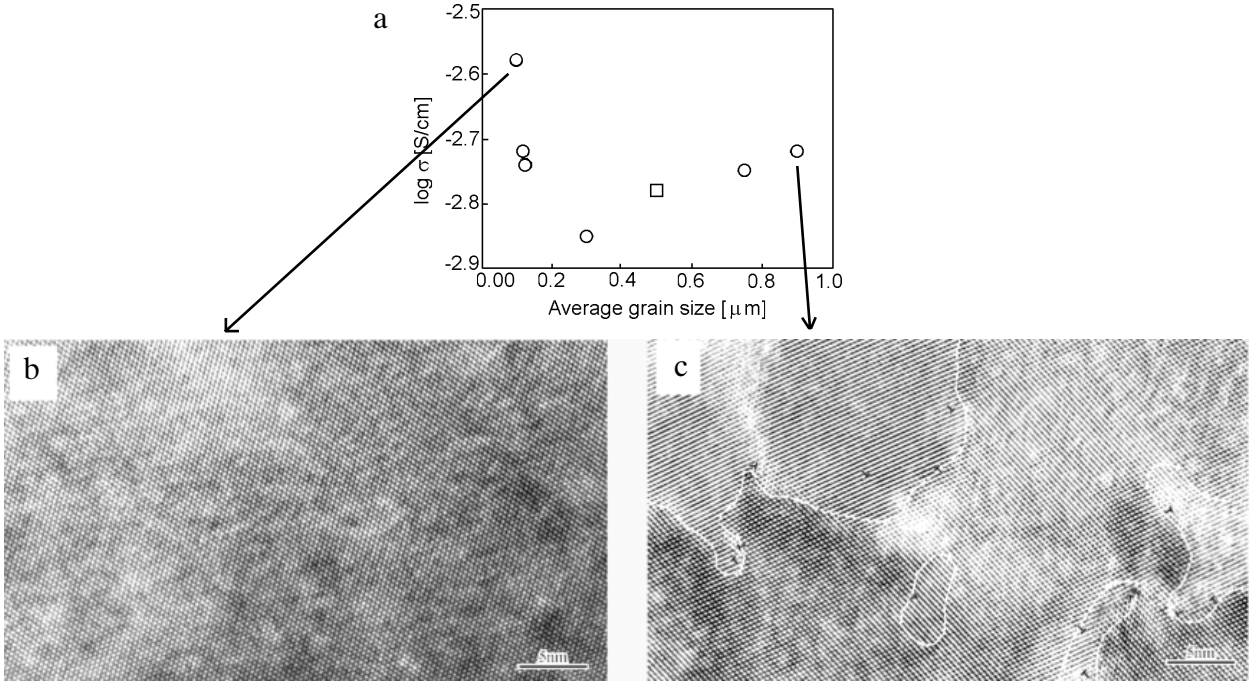

Fig. 5. (a) Grain size dependence of conductivity in $Y_{0.25}Ce_{0.75}O_{1.875}$ sintered bodies and high resolution TEM images ($<110>_F$) recorded from (b) the specimen with average grain size of 90 nm and (c) the specimen with average grain size of 0.92 μm. Dashed line area means microdomain. ⊥ symbol indicates dislocation. Ref. [18].

additional characterization such as measurement of transport number of oxygen and observation of electronic structure in doped CeO_2 using XANES analysis is required. After these characterizations, we expect that the nanostructured CeO_2 solid electrolyte with high ionic conductivity will be created in our project. And the similar relationship between nanostructural features and conducting properties was observed in Gd-, Yb-, Dy doped CeO_2 electrolytes. Accordingly, the authors believe that the design of this nanohetero structure with microdomain is a key for improvement of conducting property in the doped ceria electrolytes.

Suggested approach for improving electrolytic properties in doped CeO_2 electrolytes

As described above, the authors examined the influence of nanostructural features on conducting properties in M doped CeO_2 system (M:Gd,Sm,Y,Yb,Dy, and La) and suggested the importance of microanalysis for development of doped CeO_2 electrolytes. In this paper, we re-introduce our suggested approach for improving electrolytic properties in doped CeO_2 electrolytes. For explanation of our idea, we must remember why microdomain with ordered structure of oxygen vacancy is formed in the grain of doped CeO_2 electrolytes. In general, the trivalence cation such as Gd, Sm, Y, Yb, Dy or La is known to replace Ce^{4+} and create oxygen vacancies. It is known that segregation of dopant cations around the grain boundary region occurs as well. The big lattice distortion would be introduced into fluorite lattice by this segregation. To minimize the lattice distortion in CeO_2 lattice, the microdomain with ordered structure of oxygen vacancy would be formed in this lattice, even though segregation level is subtle. The microdomains with distorted pylochlore structure were observed in Gd doped CeO_2, Sm doped CeO_2 and Dy doped CeO_2 solid electrolytes. In the case of Y- or Yb doped CeO_2, the microdomain consisted of distorted c-type rare earth structure in the grain. And a lot of microdomains were observed within the grain (not only around grain boundary). In addition, the big microdomain would include a lot of amount of oxygen vacancy. It is because the content of dopant cation in the big microdomain is higher than that in the matrix of the doped CeO_2. In the big microdomain, a lot of amount of oxygen vacancy would be well-ordered. Accordingly, this big microdomain lowers the conductivity in the specimens. On the basis of these arguments and experimental results, the authors concluded that microdomain size and content would be controllable by a design of processing route for fabrication of nanostructured CeO_2 electrolytes. For a design of processing route, the authors examined both preparation of nanosized powders using carbonate co-precipitation method [9, 22, 23, 25, 26] and fabrication of dense sintered bodies using the spark plasma sintering (SPS) method.

To minimize the microdomain size and microdomain content in the specimen, we conclude that the nanosized round shape particles must be prepared. In our study, the preparation condition of round shape particles was examined using ammonium carbonate co-precipitation [9] and ammonium hydrogen carbonate co-precipitation method [22, 23, 25, 26]. In both methods, homogeneous precipitation could be prepared by a selection of optimum processing factors (i.e. optimum concentration of precipitant, Ce nitrate or rare earth nitrate aqueous solution, or optimum reaction temperature and time for preparation of homogeneous precipitation). The dried CeO_2 particles doped with M^{3+} (M:Gd,Sm,Y,Dy and so on) showed no appreciable morphologic changes by calcination. Both dried and calcined powders were observed to be composed of uniformly sized, round shaped, and discrete particles. The average particle sizes of both powders were 20 to 30 nm in all doped CeO_2 systems. These powders can be sintered to over 95% dense of theoretical density in the temperature range of 950°C to 1450°C using conventional sintering (CS) methods.

In order to develop high quality doped CeO_2 electrolytes, the authors proposed a combined process of SPS and CS for the design of nanostructural feature in doped CeO_2 solid electrolyte. SPS is a sintering method that allows a quick densification utilizing the microscopic electrical discharges that occur between particles that are under pressure and that are simultaneously subjected to an applied electric current. This sintering method is useful for preparation of nanostructured oxide composites. However, SPS has not been applied to fabricate the dense sintered bodies of rare earth doped CeO_2 electrolytes. The reason for this is that carbon penetration from the graphite-die into the specimen and reduction of doped CeO_2 compound by the penetrated carbon was observed to prevent the densification of the sample. To overcome this problem, the combined process of SPS and CS was used to prepare nanostructured Dy doped CeO_2 with high density using nanosized round shape particles. The conducting properties and microstructure at the atomic level of dense specimens prepared in this manner were examined with a view to finding new ways of improving the conducting properties of doped CeO_2. Figure 6 presents conducting properties and nanostructural features in $Dy_{0.2}Ce_{0.8}O_{1.9}$ [16]. The conductivity in the specimens which were obtained by CS showed the curvature around 240 nm in the grain size dependence of conductivity. The grain size dependence of conducting property in CS specimen was the same as that of other doped CeO_2 such as Gd-, Y- or Yb doped CeO_2 electrolyte. To improve the conductivity in the small grain size region around 240 nm, the combined process of SPS and CS was examined. As Fig. 6 indicates, the conductivity in the sintered body with small grain (237 nm) was drastically improved by the present combined process. Since the grain sizes of the aforementioned (SPS + CS) and CS specimens were almost the same and both specimens had high density, it is concluded that the microdomain size in (SPS + CS) specimen is much smaller than that in CS specimen. The SAEDPs and high resolution image recorded from (SPS + CS) and CS specimens agreed with this conclusion. Accordingly, it is concluded that the proposed combined process minimizes the size of microdomain

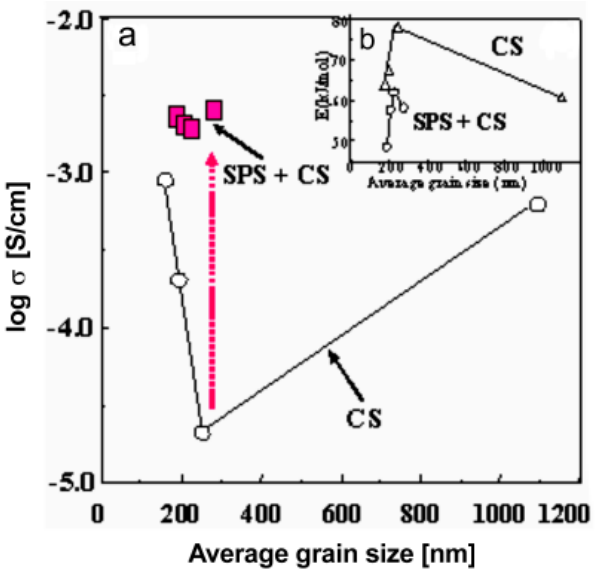

Fig. 6. Grain size dependence of (a) conductivity and (b) activation energy of $Dy_{0.2}Ce_{0.8}O_{1.9}$. Square and circle symbols in (a) indicate (SPS + CS) and CS specimens, respectively. Triangle and circle symbols in (b) indicate (SPS + CS) and CS specimens, respectively. Measurement temperature of conductivity in (a): 500°C. Temperature region for calculation of activation energy in (b): 400°C to 700°C. Ref. [16].

and improves the conducting property in the specimen. We believe that the control of micro-domain size would be a key for the development of doped CeO_2 solid electrolytes.

Conclusion

Doped CeO_2 solid electrolytes have higher conductivity than that of yttria stabilized zirconia. Doped CeO_2 electrolytes have been expected from the perspective of low temperature operation of solid oxide fuel cells. Further improvements of oxide ionic conductivity in doped CeO_2 electrolytes will be required, although the examination of the other relevant properties such as mechanical strength, thermal stability, and coefficient of thermal expansion, etc. are important from the perspective of practical use. For creation of high quality electrolytes, the strategy of development is more important. Previously reported papers have outlined the strategies to develop high performance ion conductors with related fluorite structures. But such attempt lacks an approach of microanalysis at atom level for development of ionic conductors. In the present study, the authors introduced our recent data for the microanalysis in the doped CeO_2 solid electrolytes and suggested our research plan for a design of nanostructural features in doped CeO_2 for low temperature operation of fuel cells. The authors strongly pointed out that important hint for the development of high quality solid electrolytes hides itself in the nanostructure of solid electrolytes. To develop the high quality solid electrolytes, the true nanolevel structure in the solid electrolytes should be taken into account. It is concluded that both atom level analysis and processing route design clarify a new conduction pathway in the electrolytes and provides us an opportunity for development of superior quality solid electrolytes in SOFCs.

Acknowledgment The present work was supported (in part) by the Grant-in-Aid for Scientific Research on Priority Area, "Nanoionics (439)" by the Ministry of Education, Culture, Sports, and Technology.

References

1. Buchanan R, Mori T, Wang Y, Ou DR, Drennan J (2006) Fabrication of dense $Gd_xCe_{1-x}O_{2-x/2}$ sintered bodies with nano-size grain and its conducting properties. Mater Trans Japan 30;4:955–958
2. Buttler V, Catlow CRA, Fender BEF, Harding JH (1983) Dopant ion radius and ionic conductivity in cerium dioxide. Solid State Ionics 8:109–113
3. Eguchi K, Kunisaki T, Arai H (1986) Effect of microstructures on the ionic conductivity of ceria-calcia oxides. J Am Ceram Soc 69;11:C282–C285
4. Gerhart R, Nowick AS (1986) Grain-boundary effect in ceria doped with trivalent cations: I. Electrical measurement. J Am Ceram Soc 69;9:641–646
5. Gerhart R, Nowick AS, Mochel ME, Dumler I (1986) Grain-boundary effect in ceria doped with trivalent cations: II. Microstructure and microanalysis. J Am Ceram Soc 69;9:647–651
6. Hamakawa S, Hayakawa T, York APK *et al*. (1996) Selective oxidation of propene using an electrochemical membrane reactor with CeO_2 based solid electrolyte. J Electrochem Soc 143;4:1264–1268
7. Hong SJ, Mehta K, Virkar AV (1998) Effect of microstructure and composition on ionic conductivity of rare-earth oxide doped ceria. J Electrochem Soc 145;2:638–647
8. Kilner J (2000) Fast oxygen transport in acceptor doped oxides. Solid State Ionics 129:13–23
9. Li JG, Ikegami T, Mori T, Wada T (2001) Reactive $Ce_{0.8}Re_{0.2}O_{1.9}$ (Re=La,Nd,Sm,Gd,Dy,Y,Ho,Er, and Y) powders via carbonate precipitation. 1. Synthesis and characterization. Chem Mater 13;9:2913–2920
10. Minh NQ (1993) Ceramic fuel cells. J Am Ceram Soc 76;3:563–588
11. Mori T, Drennan J, Lee JH, Li JG, Ikegami T (2002) Oxide ionic conductivity and microstructure of Sm or La doped CeO_2 based system. Solid State Ionics 154/155:461–466
12. Mori T, Drennan J, Wang Y, Auchterlonie G, Li JG (2004) Influence of nanostructural features on electrolytic properties of Gd doped CeO_2 solid electrolytes. J Ceram Soc Jpn 112;5:S642–S648
13. Mori T, Drennan J, Wang Y, Auchterlonie G, Li JG, Yago A (2003) Influence of nanostructural feature on electrolytic properties in Y_2O_3 doped CeO_2 system. J Sci Technol Adv Mater 4:213–220
14. Mori T, Drennan J, Wang Y, Lee JH, Li JG, Ikegami T (2003) Electrolytic properties and nanostructural feature in La_2O_3-CeO_2 system. J Electrochem Soc 15;6:A665–A673
15. Mori T, Drennan J, Wang Y, Li JG, Ikegami T (2002) Influence of nanostructure on electrolytic properties in CeO_2 based system. J Therm Anal Calorim 70:309–319
16. Mori T, Kobayashi T, Wang Y *et al*. (2005) Synthesis and characterization of nanohetero-structured Dy doped CeO_2 solid electrolytes using combination process of spark plasma sintering and conventional sintering. J Am Ceram Soc 88;7:1981–1984

17. Mori T, Wang Y, Drennan J, Auchterlonie G, Li JG, Ikegami T (2004) Influence of particle morphology on nano-structural feature and conducting property in Sm-doped CeO_2 sintered body. Solid State Ionics 175:641–649
18. Ou DR, Mori T, Ye F, Takahashi M, Zou J, Drennan J (2006) Microstructures and electrolytic properties of yttrium-doped ceria electrolytes: dopant concentration and grain size dependence. Acta Mater (in press)
19. Riess I, Braunshtein D, Tannhauser DS (1981) Density and ionic conductivity of sintered $(CeO_2)_{0.82}(GdO_{1.5})_{0.18}$. J Am Ceram Soc 64;8:479–485
20. Singman D (1966) Preliminary evaluation of ceria-lanthana as a solid electrolyte as a solid electrolyte for fuel cell. J Electrochem Soc 113;5:502–505
21. Steel BCH (2001) Materials for fuel-cell technologies. Nature 414;15:345–352
22. Wang Y, Mori T, Drennan J, Li JG, Yajima Y (2004) Low temperature synthesis of 10 mol% Gd_2O_3-doped CeO_2 ceramics and its characterization. J Ceram Soc Jpn 112;5:S41–S45
23. Wang Y, Mori T, Li JG (2006) Synthesis, characterization and sinterability of 10 mol% Sm_2O_3-doped CeO_2 nanopowders via carbonate precipitation. J Eur Ceram Soc 26;4/5:419–422
24. Wang Y, Mori T, Li JG, Drennan J (2005) Synthesis, characterization, and electrical conduction of 10 mol% Dy_2O_3-doped CeO_2 ceramics. J Eur Ceram Soc 25:949–956
25. Wang Y, Mori T, Li JG, Ikegami T, Yajima Y (2003) Low-temperature preparation of dense 10 mol%-Y_2O_3-doped CeO_2 ceramics using powders synthesized via carbonate co-precipitation. J Mater Res Soc 18;5:1239–1246
26. Wang Y, Mori T, Li JG, Yajima Y (2003) Low-temperature fabrication and electrical property of 10 mol% Sm_2O_3-doped CeO_2 ceramics. J Sci Technol Adv Mater 4:229–238
27. Yahiro H, Baba Y, Eguchi K, Arai H (1988) High temperature fuel cell with ceria-yttria solid electrolyte. J Electrochem Soc 135;8:2077–2080
28. Yamamoto O (2000) Solid oxide fuel cells: fundamental aspects and prospects. Electrochim Acta 45;15/16:2423–2435
29. Yamazoe N, Miura N (1999) Gas sensors using solid electrolytes. MRS Bull 24;6:37–43
30. Ye F, Mori T, Ou DR, Takahashi M, Zou J, Drennan J (2006) Influence of microstructure on ionic conductivity of ytterbium doped ceria. J Am Ceram Soc (in press)